Journal of The Electrochemical Society, **158** (4) C104-C110 (2011)
0013-4651/2011/158(4)/C104/7/$28.00 © The Electrochemical Society

Transpassive Dissolution of Copper and Rapid Formation of Brilliant Colored Copper Oxide Films

N. Fredj and T. D. Burleigh[*,z]

Materials and Metallurgical Engineering Department, New Mexico Tech, Socorro, New Mexico 87801, USA

This paper describes an electrochemical technique for growing adhesive copper oxide films on copper with attractive colors ranging from gold-brown to pearl with intermediate colors from red violet to gold green. The technique consists of anodically dissolving copper at transpassive potentials in hot sodium hydroxide, and then depositing brilliant color films of Cu_2O onto the surface of copper after the anodic potential has been turned off. The color of the copper oxide film depends on the temperature, the anodic potential, the time t_1 of polarization, and the time t_2, which is the time of immersion after potential has been turned off. (At potentials lower than the transpassive region, that is, in the passive region, the oxide film is a dark gray or dark green matte with a blue powder hydroxide on the surface and it is not attractive.) The brilliant colored films were characterized using glancing angle x-ray diffraction, and the film was found to be primarily Cu_2O. Cyclic voltammetry, chronopotentiometry, scanning electron microscopy, and x-ray photoelectron spectroscopy were also used to characterize these films. These techniques show that the different colors were due to differences in porosity and thickness rather than changes in composition.
 [DOI: 10.1149/1.3551525]

Manuscript submitted September 14, 2010; revised manuscript received January 10, 2011. Published February 28, 2011.

Copper and its alloys are unique in being the only nongray colored metals, other than gold and its alloys. Polished copper is a warm, reddish-brown color, and its surface color can change depending upon the exposure time and environment. The colored surface films (patina) that form on copper alloys are of particular interest to the fields of architecture and sculpture art. A copper office complex in Amsterdam, the Netherlands, was given a brown chocolate patina by progressive oxidation of the copper, while copper warehouses in Hamburg, Germany, became an almond green patina after many years in outdoor atmospheric exposure.[1]

Copper has been widely studied, and there are many chemical techniques for coloring copper. Taguri et al. developed attractive colored finishes for copper and copper alloys by simply immersing the metal in a selenious acid solution of controlled concentration and *p*H at room temperature and they grew films with thicknesses between 10 and 70 nm, but these films were not stable in the atmosphere and had to be protected by a layer of clear lacquer. Taguri et al. showed that the colors were due to interference effects.[2] Miley oxidized copper by heating samples in an electric furnace at different temperatures. These colors varied from dark brown to silvery green with intermediate colors like red-brown, violet, or blue with an average thickness of tens of nanometers. Miley also showed that the cuprous–cupric oxide layer contained an intimate mixture of the two oxides or possibly a solid solution with the greater concentration of the cupric oxide toward the outer surface and the cuprous oxide toward the base metal. Light could be reflected from the outer and inner surfaces of the cuprous–cupric oxide film, and exhibit interference effects, unless a separate layer of cupric oxide grew over it.[3] Recently Allred described a method to build a rainbow by electrodepositing a cuprous oxide on glass at different times by deposition of thin films.[4] The nanoscale thickness of the film, which correlated to the color, was varied by changing the deposition time. The coloration is proposed to originate from iridescence, i.e., constructive interference of light reflected at the outer air/oxide and the inner oxide/metal interfaces.[5,6]

The electrochemical behavior of copper in alkaline media has been extensively studied, but mostly in dilute alkaline solutions.[7–9] A few studies had been conducted in the concentrated alkaline solutions.[10–12] Biton et al. studied the behavior of copper in 45% KOH solution between −0.4 and 0.6 V/standard hydrogen electrode (SHE), but only at ambient temperature. In this potential range, they showed that the major surface oxide formed on copper at potential P_1 (−0.34 V/SHE) was Cu_2O. Further polarization to the potential P_2 (−0.07 V/SHE) led to the precipitation of surface films comprising of two layers, $Cu_2O/Cu(OH)_2$, where Cu_2O was the inner layer, and $Cu(OH)_2$ was the light blue, dusty precipitate. They reported that the copper was oxidized only to Cu_2O (rather than to CuO) because the charge transfer occurred through surface films, which limited the oxidation power of the electrode.[12] Biton et al. focused on the lower passive potentials which corresponded to the two major anodic peaks in the voltammogram. It is also possible to deposit Cu_2O from acidic or weakly acidic solutions containing Cu^{2+} cations, but that is a different field.[13]

In this paper, we describe the electrochemical growth of copper oxide in hot concentrated sodium hydroxide by the polarization of the copper at transpassive potentials. Our objective is to grow an aesthetic and adherent oxide film on copper and to understand the growth mechanism and the effect of temperature, potential, and time.

Experimental

Materials.—The cold-rolled polycrystalline copper test sheet was 96.6Cu–2.47Ni–0.5Si–0.17Mg–0.14Zn–0.03Sn–0.06Fe–0.01Al–0.01Mn (the composition is given in weight percent), with a thickness of 0.32 mm. The test electrolyte was 50% W/W NaOH, (19 M, $p\mathrm{H} = 15.3$) from Ricca Chemical Company, Arlington, TX. The 50% W/W solution prepared by adding 760 g NaOH to 760 g H_2O to make about 1 liter of solution. The electrolyte temperatures were 25, 45, 65, and 85°C and potential was applied using a TecNu DCa 25/12-1Z power supply with two copper electrodes, from +1 to +5 V (versus the copper cathode). The reference electrode was Ag/AgO/NaOH made by anodizing silver sheet in 19 M NaOH at +3 V versus Ag and at 45°C until black. The black silver sheet was then encapsulated in a tube containing 19 M NaOH, with a fritted glass seal between the silver and the anodizing electrolyte. The purpose of using the Ag/AgO/NaOH reference electrode instead of a Calomel electrode was to prevent chloride contamination of the anodizing solution.

The copper sheet was cut into 3 cm × 7 cm rectangles, and degreased by wiping first with acetone and then with methanol, and then only the lower half of the sample was immersed (3 cm × 3 cm) in the solution. Although both sides of the sample were anodized, the results are given only for the front surface. This report describes the tests conducted on this copper sheet, but similar results were found for other copper samples and also for alloys of copper. Tests were conducted on as-received copper sheet, and on copper polished to 1 μm Al_2O_3 or diamond.

Anodic polarization of the copper.—Prior to each test, the sodium hydroxide solution was gradually heated to the designated temperature while being stirred at 150 rpm on a hot plate. When the

* Electrochemical Society Active Member.
z E-mail: burleigh@nmt.edu

electrolyte temperature was stable, two identical samples of copper (one the anode and the other one the cathode) were immersed in the electrolyte with a separation of 7 cm and then a potential of +3, +4, or +5 V was applied for a time of t_1 which varied from 5 to 60 s, but was typically 10 s. During time t_1, the positive copper was anodically polarized into the transpassive region, and several reactions occurred. Initially the copper surface darkened as the oxide thickened. However, after several seconds, a dissolution front was seen moving across the surface, stripping off the oxide, and leaving bare copper and oxygen evolution. At the end of time t_1, the potential was returned to zero, and the sample was left immersed in the solution for a time of t_2, which varied from zero to hundreds of seconds. During time t_2, the color of copper changed gradually due to the growth of copper oxide on the activated copper surface. If the copper was removed immediately ($t_2 = 0$ s), then its color would be that of bare copper. If the copper remained immersed for a longer time in the electrolyte, the copper oxide color would be completely different. Therefore, the four key experimental parameters, in addition to the copper composition and the electrolyte concentration, were: (1) anodic potential, (2) temperature, (3) t_1 = time of anodic polarization, and (4) t_2 = time of growth of oxide after anodization. At the end of time t_2, the sample was removed from solution, rinsed with deionized water, and then dried with compressed air.

The anodic polarization started with a new clear solution of 19 M NaOH at each temperature, and during the applied potential the solution initially turned gray and then blue (Cu^{2+} and $HCuO_2^-$ ions). During these tests, the electrolyte became saturated or supersaturated with the copper ions.

Characterization techniques.—Cyclic voltammetry tests were conducted between −1.5 and +1.5 V versus Ag/AgO/NaOH at different temperatures (25, 45, 65, and 85°C) stirred in 19 M NaOH and the current density versus potential is recorded with a PARSTAT 2263 potentiostat running PowerSuite software. The scan rate was 20 mV/s and the immersed surface was about 1 cm^2.

Chronopotentiometry was used for measuring the thickness of the oxide film for the different conditions of growth. The chronopotentiometry was conducted using a PARSTAT 2263 potentiostat running PowerSuite software. The colored copper samples were immersed in a 0.2 M ammonium chloride solution and reduced at ambient temperature at a constant current 100 μA for 0.64 cm^2 and the potential was recorded with time. This method was utilized by Miley in 1937 and may be used to calculate the thickness of an oxide.[3] The time required for the cathodic reduction of the oxide is multiplied by the current density to give the Q, coulombs of electricity consumed per cm^2. The thickness in nanometers may be calculated by using Eq. 1 where the conversion factor K, equals 1236 for Cu_2O, or 639 for CuO

$$\text{thickness (nm)} = Q \times K \quad [1]$$

The surface morphology of copper oxide was studied using a Hitachi S-800 field emission scanning electronic microscope (FESEM) at an accelerating voltage of 20 kV. Raman measurements were carried out on a LabRAM Raman microscope (HORIBA Jobin Yvon Inc., NJ). Laser intensities at the samples were set at approximately 130 μW for the 632.8 nm HeNe laser. Between different Raman sessions, the 520.7 cm^{-1} peak of a silicon wafer was used to calibrate the spectrograph for possible fluctuation of the Raman system. Exposure time for all measurements was 1 s. Each spectrum was the average of 10 scans.

X-ray photoelectron spectroscopy (XPS) was collected by a ThermoScientific ESCALAB 250 x-ray Photoelectron Spectrometer at the University of Oregon. The pass energy was about 150 eV for survey scans and 20 eV for "multiplex" scans. The source was a monochromatic Al x-ray (1486.6 eV photon energy) with a spot size about 400 μm and 1 kV 1 μA Ar^+ beam was used for sputtering.

Glancing-angle x-ray diffraction (GAXRD) patterns were obtained using X'PERT-PRO diffractometer at the New Mexico Bureau of Geology and Mineral Resources. The x-ray diffraction (XRD) diffractometer had a thin film attachment, unfiltered Cu-Kα radiation and a glancing incidence angle of 0.8° and a step size about 0.02°.

Results and Discussion

Synthesis of aesthetic copper oxide films.—Reproducible copper oxide films were obtained by controlling the electrolyte composition (19 M NaOH), the electrolyte temperature (T), the applied potential (E), the dissolution time during the applied anodic potential (t_1), and the time for growth of the oxide after the anodic potential was terminated (t_2). The possible combinations of these five parameters are very numerous and not the aim of this work. In this paper, the results are limited to the three parameters E, T, and t_2. Figure 1 shows an example of a typical coating run. Table I demonstrates the color map for $t_1 = 10$ s and $t_2 = 60$ s, and for different applied potentials E and temperatures T. Figure 2 shows examples of the different esthetic colors. We believe that this is the first report on the role of time t_2 together with potential and temperature on the resulting color, thickness, and porosity of the films.

For a given times t_1 and t_2, there were three distinct domains as shown in Table I. The first domain was the passive region where there was very little dissolution and deposition of the oxide. This passive region existed at temperatures lower than 45°C and potentials lower than +1 V versus the copper cathode. The second domain existed from 65 to 85°C, and between +1 and +2 V versus copper, and for this domain the oxide film was a homogenous, thick, dark, nonaesthetic gray or green matt, and the current density during t_1 was very small. Notable in this region is a light blue precipitate of $Cu(OH)_2$ which deposited onto the surface of the oxide previously reported by Biton et al.[12] In the third domain, at all temperatures and for potentials $E_3 = +3$ V, $E_4 = +4$ V, and $E_5 = +5$ V versus copper, the deposited film had a large range of colors which were a function of the temperature and t_2. The color evolved from gold brown at room temperature, to brown reddish, violet blue, blue violet, green blue, green gold, and finally to pink and pearl at 85°C. In the potential range +3 to +5 V versus copper, the color was bright, esthetic and nonspalling (contrary to the oxides formed in furnaces at high temperatures[14]). The color was nonuniform, with the oxide slightly thicker along the sample edges compared to the center. This evolution of color and thickness was also dependent on t_2. At $t_2 = 60$ s, a sample was violet-blue, but with longer t_2 the film became blue-violet (more blue) due to longer contact with the solution, which gave more time for a thicker deposits, and consequently a deeper color. Parameter t_2, the time after the applied potential is

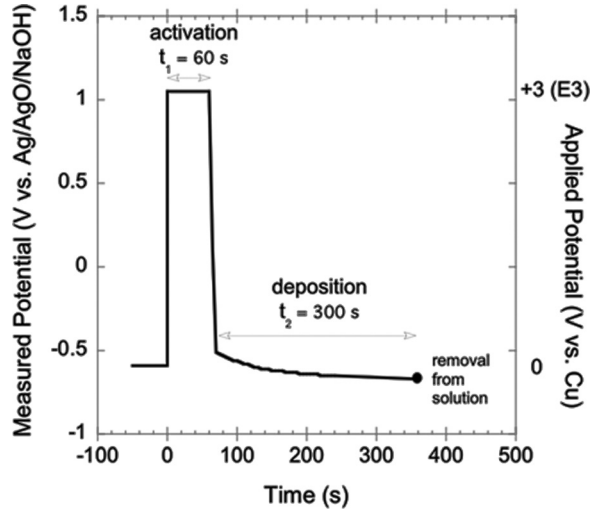

Figure 1. Experimental procedure for growing the copper oxide films.

Table I. Color of copper oxide film with $t_1 = 10$ s and $t_2 = 60$ s. P = $Cu(OH)_2$ precipitate.

°C	+1 V	+2 V	+3 V	+4 V	+5 V
85	Dark gray	Dark green+blue P	Pink	Pearl	Pearl
65	Dark gray	Dark green+blue P	Green-gold	Green-gold	Green-gold
45	Ø	Dark green+blue P	Violet-blue	Blue-violet	Blue-violet
25	Ø	Ø	Gold	Gold-brown	Gold-brown

shut off, is the dominant parameter that determines the color and thickness of the oxide film.

Electrochemical domains.—Cyclic voltammetry was used in order to understand the electrochemical behavior of the copper in the 19 M NaOH and to identify the different potentials of oxidation. The copper was polarized from –1.5 to +1.5 V versus Ag/AgO at four different temperatures (25, 45, 65, and 85°C), and the results are shown in Fig. 3. Figure 3a is a voltammogram at 25°C, and it shows two anodic peaks (a_1 and a_2) and one cathodic peak (c_1). During the positive sweep, the copper Cu^0 is oxidized at −590 mV into Cu_2O (Cu^I peak a_1). Because of the low conductivity of Cu_2O, the peak a_1 is much smaller than a_2.[8,15] The peak a_2 around −210 mV might be due to the oxidation of Cu^0 into Cu^{II} to form the Cu_2O/CuO/$Cu(OH)_2$, a triplex film described by Kunze.[16] Between 0 and +500 mV, the copper is in the passive domain and the higher potentials belong to transpassive state. The potentials +1, +2, +3, +4, and +5 V versus the copper cathode are represented in the Fig. 3 by E_1, E_2, E_3, E_4, and E_5 versus Ag/AgO. Potential E_1 lies just after the peak a_1 where Cu_2O is reported to be the main oxide. Potential E_2 lies in the passive region for CuO and $Cu(OH)_2$ after the second peak a_2, and potentials E_3, E_4, and E_5 are all in the transpassive region. When the potential increases, $Cu(OH)_2$ is reported to be transformed into CuO.[8,15]

In the cathodic sweep (dashed curve) in Fig. 3a, near −1 V, there is a large peak c_1 which represents a reduction of Cu^{II} and Cu^I to Cu^0. Also in the cathodic sweep, between −0.50 and 0 mV, an anodic peak A appears with the similar current as the anodic sweep peak a_1. The appearance of this anodic peak during the negative sweep in strong alkaline media has previously been reported. Recently, Lorimer et al. reported that an oxidative current can be seen on the reverse sweep under both ultrasound and silent conditions, and suggests that the passivating coating was removed by reduction while the electrode was still at pronounced oxidizing potential, allowing further copper oxidation to occur.[10] Other authors had the same report[17–19] but still found this unusual peak to be controversial. However, from a corrosion science viewpoint, it is apparent that copper is an active–passive metal in this electrolyte and temperature, and peak A is an active dissolution peak.

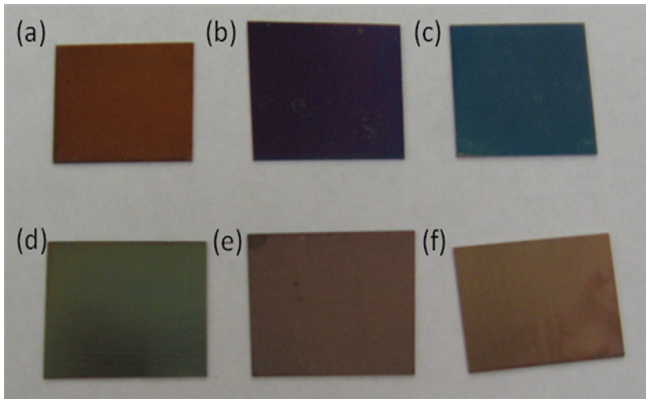

Figure 2. (Color online) Colors of copper oxide films. (a) gold-brown, (b) violet-blue, (c) blue, (d) gold-green, (e) pink, and (f) pearl.

At 45°C, in Fig. 3b, the cyclic voltammogram becomes more complicated, and the active peak, A, becomes narrower and shifted to higher potentials. Figure 3b is similar to Fig. 3a, but E_1 is now at the onset of a_2 and E_2 is in the passive region, and E_3, E_4, and E_5 all are in the transpassive region. At −1 V, there is still a broad reduction peak, c_1.

At 65°C in Fig. 3c, in the positive sweep, peak a_1 is near −0.6 V and peak a_2 is near −0.33 V. There is now a new peak a_3 at 0.35 V, just prior to the transpassive region, which might be the oxidation of copper Cu^0 to Cu^{III} (Cu_2O_3).[8] In the negative sweep, there is a small reduction peak c_3 for Cu_2O_3 at +0.16 V. At lower potentials, c_1 has split into two reduction peaks, c_2 and c_1, which represents the reduction of Cu^{II} to Cu^I and Cu^I to Cu^0. At 85°C in Fig. 3d, the voltammogram is similar to 65°C, but reduction peaks c_1, c_2, and c_3 are more pronounced.

Noteworthy is that the cyclic voltammetry demonstrated the potentials E_3, E_4, and E_5 (+3 V, +4 V, and +5 V versus the copper cathode, the potentials for the attractive colors), all belong to a transpassive domain at all of the studied temperatures (25, 45, 65, and 85°C). Voltammetry also indicated that as the temperature increased, the potential E_2 moved closer to the transpassive region, and the broad peaks deconvoluted into double peaks, and an additional oxidation peak a_3 and reduction peak c_3 appeared for the Cu^{III}.

Determination of thickness by using chronopotentiometry.—Effect of potential.— Some of the copper oxide films were cathodically reduced in order to determine their thicknesses. Figure 4 shows that cathodic chronopotentiograms recorded for four oxides grown anodically (+1, +2, +3, and +5 V versus copper) at 65°C, with $t_1 = 10$ s and $t_2 = 60$ s. These reduction curves show only one potential plateau near −0.3 V versus Ag/AgO whereas the +2 V sample (with blue precipitate of hydroxide copper on the surface) shows two plateaus, C_I and C_{II}. The larger plateau for all cases most likely corresponds to the equilibrium between cuprous oxide Cu_2O (Cu^+) and metallic copper Cu. At +2 V, the small plateau C_I corresponds to the equilibrium between $Cu(OH)_2$ (Cu^{2+}) and Cu_2O (Cu^+). The chronopotentiometry results also show that for +3, +4 (not shown), and +5 V, less time is required to reduce Cu_2O into copper than for +1 and +2 V, which implies that the thickness of oxide decreased. These thicknesses were calculated with Eq. 1 and are shown in Fig. 5. The oxide is assumed to be Cu_2O, which will be confirmed in Sec. V on XRD. The oxides formed at +3, +4, and +5 V have a similar thickness (≈50 nm) and a similar color (green gold). Some of the chronopotentiograms (see the zoom in Fig. 4b) show a small potential peak which might be due to the reduction of residual cuprous oxide CuO at the copper interface.

The decrease in thickness with an increase in anodic potential has also been observed by He et al.[19] for copper, but this is opposite to the general trend for metals.[20] The thickness of the anodic oxide on most metals typically increases with potential, for example, magnesium,[21] titanium,[14,20,22,23] tantalum,[24] aluminum,[23,25] and also copper.[26] The explanation for copper in 19 M NaOH is that at +3 V and higher, the copper dissolution rate exceeds the passive film growth rate, so there is no significant anodic oxide on the surface.

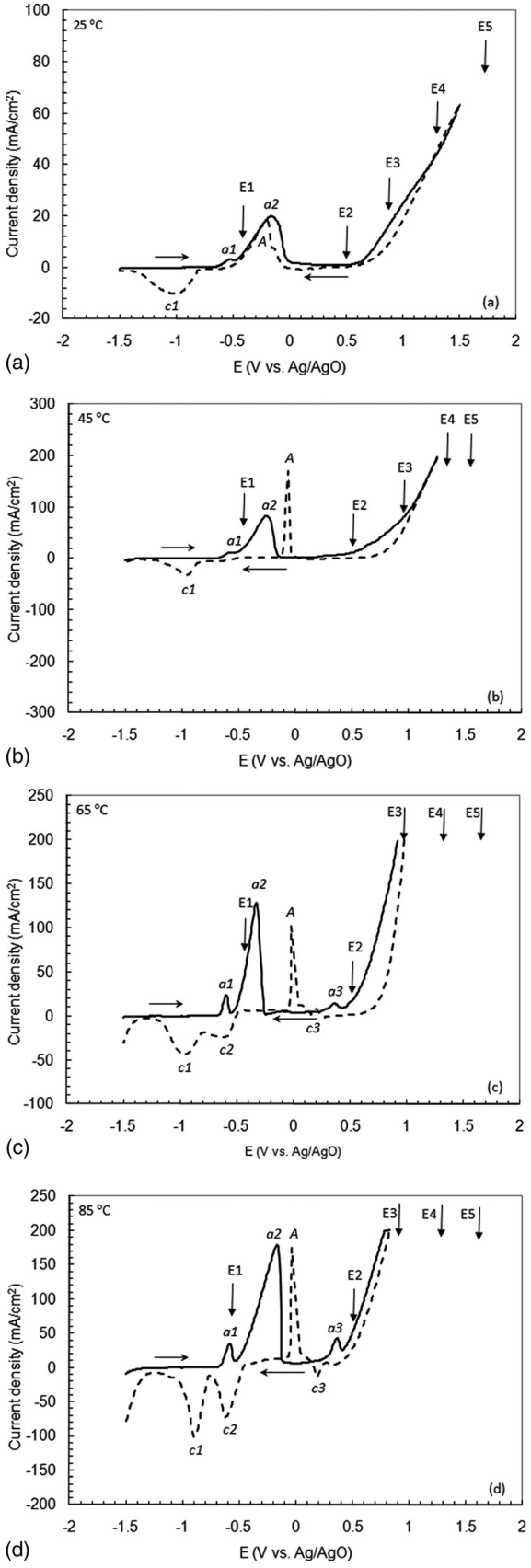

Figure 3. Cyclic voltammogram of a polycrystalline copper in 19 M NaOH (scan rate = 20 mV/s): (a) 25°C, (b) 45°C, (c) 65°C, and (d) 85°C. The potentials +1, +2, +3, +4, and +5 V vs the copper cathode are labeled as E_1, E_2, E_3, E_4, and E_5 in the graphs.

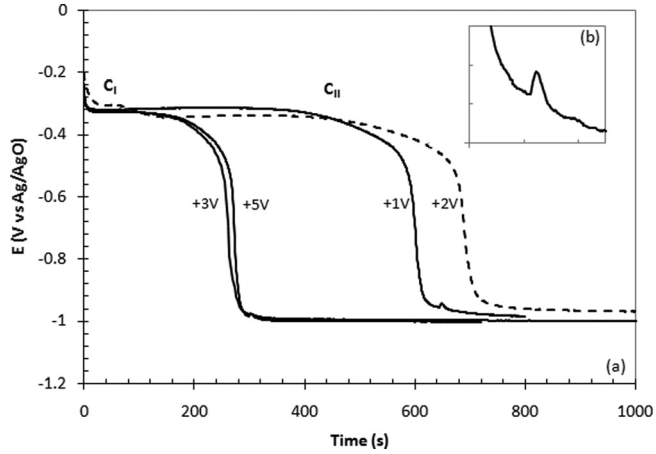

Figure 4. Chronopotentiograms of oxidized copper at different potential (+1, +2, +3, and +5 V vs copper) at 65°C with $t_1 = 10$ s and $t_2 = 60$ s (a) and a zoom (b).

This will be discussed further during the scanning electron microscope (SEM) results.

Effect of temperature.—The chronopotentiometry was used to determine the effect of temperature on the thickness of oxide copper. Figure 6a shows the evolution of thickness for samples anodized at +3 V versus copper (transpassive region) with $t_1 = 10$ s and $t_2 = 60$ s for temperatures from 25 to 85°C. The thickness increases with temperature from 10 to 100 nm, which means that the growth of oxide is an activated phenomenon. The insert in Fig. 6b demonstrates that the thickness fits the Arrhenius law with activation energy of 33 kJ/mol, which is similar to the results of Jackson[27] and Demir et al.[28] In addition, each temperature is associated with a different color from gold to pink, which means that the appearance of film is a consequence of the thickness of the oxide.

Effect of t_2.—Figure 7 shows the evolution of the thickness of Cu_2O versus t_2 as determined by chronopotentiometry. The films were grown at 45°C, +3 V, $t_1 = 10$ s and varying t_2. The evolution shows two regimes. The first regime exists from 0 to 120 s where the thickness increases almost linearly from 7 to 61 nm. In this time domain, each t_2 is associated with a different color. When the t_2 increases, the color of copper oxide varies from bare copper to green with intermediate colors of brown reddish and blue. Beyond 120 s, the thickness of Cu_2O is stable at about 75 nm and the color no longer

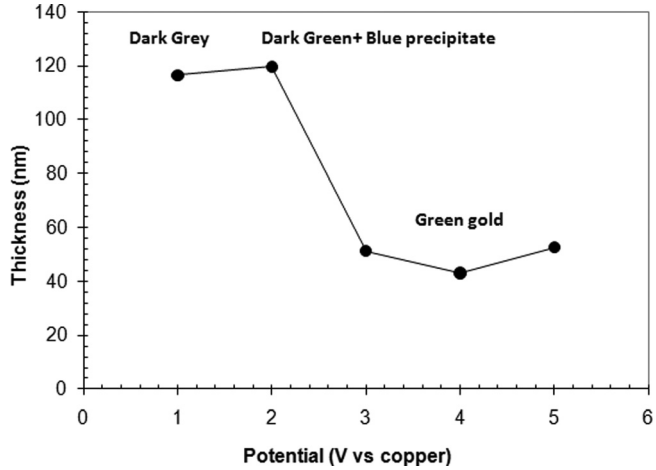

Figure 5. Evolution of thickness of cuprous oxide Cu_2O polarized at 65°C with $t_1 = 10$ s and $t_2 = 60$ s at different potentials on reduction using chronopotentiometry.

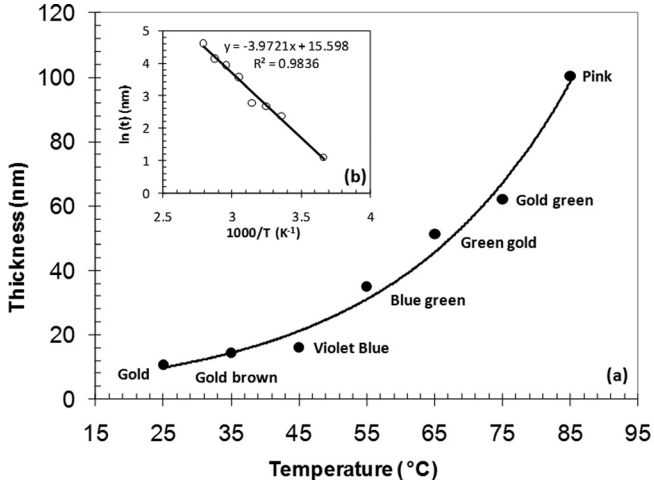

Figure 6. Evolution of thickness (t) of Cu_2O films based on the reduction using chronopotentiometry (+3 V vs copper with $t_1 = 10$ s and $t_2 = 60$ s) (a) and identification of Arrhenius behavior (b).

changes. In summary, the growth of the copper oxide during t_2 is initially rapid and almost linear until it reaches a constant thickness and color. The time will depend on the concentration of the copper ions in the NaOH electrolyte.

SEM surface characterization.—Effect of potential.—Figure 8 shows the surface oxide at 65°C with $t_1 = 10$ s and $t_2 = 60$ s polarized at different potentials (+1, +2, +3, and +5 V versus the copper cathode). Figure 8 reveals that the morphology of copper oxide is strongly dependent on the potential. At +1 V versus copper (E_1), shown in Fig. 8a, the surface is partially covered by pyramids, which is the typical shape of Cu_2O.[29,30] This Cu_2O shape is dependent also on the potential and *p*H.[31] The presence of Cu_2O was also confirmed with cyclic voltammetry (Fig. 3c) because E_1 was after the first peak of anodization (a_1). Assuming the oxide is Cu_2O, the thickness at +1 V would be 120 nm (Fig. 5).

In Fig. 8b, at +2 V, there is a formation of a light blue precipitate on the surface of the dark oxide with random needles, which is the copper hydroxide, $Cu(OH)_2$.[12,29] If the $Cu(OH)_2$ is wiped away, a darker oxide is present beneath it.

In Figs. 8c and 8d, at +3 V, +4 V (not shown), and +5 V, the oxides have a green gold color and the SEM appearance of the oxides is similar. They have a thickness about 50 nm (Fig. 5) assuming Cu_2O.

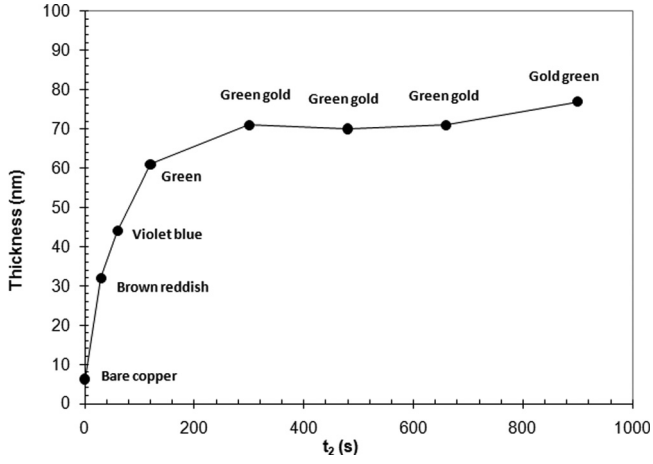

Figure 7. Evolution of thickness (t) of Cu_2O films based on reduction using chronopotentiometry (+3 V vs copper, T = 45°C with $t_1 = 10$ s).

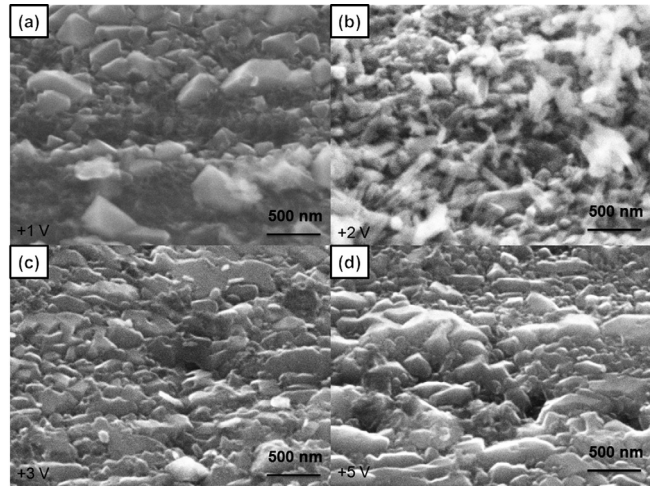

Figure 8. Evolution of the surface morphology for copper polarized at 65°C with $t_1 = 10$ s and $t_2 = 60$ s:(a) +1 V/ dark gray, (b) +2 V/dark green with a blue precipitate $Cu(OH)_2$, (c) +3 V/green-gold, and (d) +5 V/green-gold.

Effect of temperature.—Figure 9 shows the evolution of the copper oxide surface at temperatures (25, 45, 65, and 85°C) and at a constant potential of +3 V versus copper (E_3). At the room temperature (Fig. 9a), the clumps of particles appear to be Cu_2O based on their shape. At 45°C (Fig. 9b), the Cu_2O grows thicker (seen in Fig. 6) but the oxide is porous and rough. At 65°C the thickness increases and surface becomes less porous. At 85°C, the oxide grows in thickness, and large plate precipitates appear on the surface (Fig. 9d).

Effect of t_2.—Figure 10 shows an example of the microstructure of two samples anodized under the same conditions (45°C, +3 V, and $t_1 = 60$ s) but with $t_2 = 60$ and 900 s. The color was different, being violet blue for the shorter time and gold green for the longer time. With the shorter time after anodization (Fig. 10a), the microstructure has higher porosity and roughness, whereas at longer times (Fig. 10b), the surface is smoother, which agrees with ellipsommetry measurements (not shown). Consequently during anodization the surface is activated and ions Cu^{2+} dissolve into the sodium hydroxide. When the anodization is stopped, the sample is still in contact with the solution and the deposition of copper oxide occurs. For short times, the surface oxide is thin and rough, while for longer times, the copper oxide is thicker and more uniform.

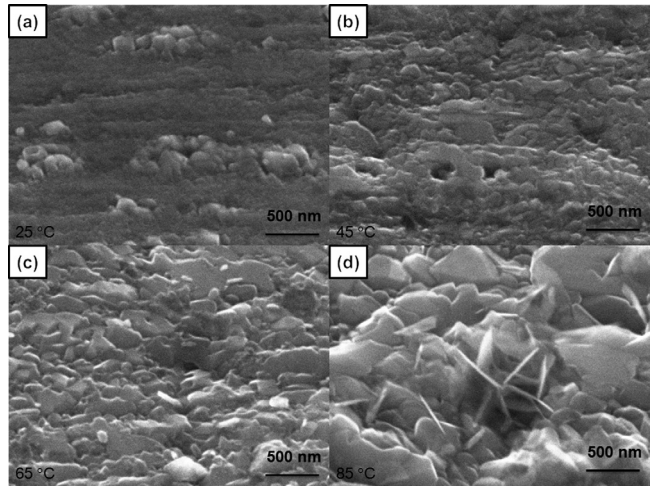

Figure 9. Evolution of morphology for surface oxide polarized at +3 V (E_3) with $t_1 = 10$ s and $t_2 = 60$ s: (a) 25°C/gold, (b) 45°C/violet-blue, (c) 65°C/green-gold, (d) 85°C/pink.

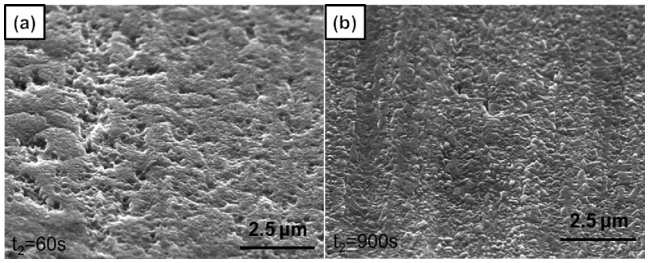

Figure 10. Evolution of morphology of surface of oxide copper anodized at 3 V and 45°C with $t_1 = 60$ s (a) $t_2 = 60$ s/violet-blue, (b) $t_2 = 900$ s/gold-green.

XRD characterization of the copper oxide.—Figure 11 shows the glancing angle XRD spectra for copper polished to 1 µm diamond and then polarized at 65°C with $t_1 = 10$ s and $t_2 = 60$ s for potentials +1, +2, +3, and +5 V versus copper. The spectrum for +4 V is not shown, but is similar to +3 and +5 V. The XRD spectra for the bare copper and at +1, +3, +4, and +5 V versus copper show two large peaks at 43 and 51°, which belong to the copper substrate, a cubic system with a lattice parameter a = 0.36247 nm (ICSD[32] card 01-070-3038). At +1, +3, +4, and +5 V (all potentials except +2 V), the oxide is predominantly cuprous oxide Cu_2O, a cubic system with a lattice parameter a = 0.42580 nm (ICSD[32] card 01-077-0199), based on the peaks at 30, 37, 42, and 62°. At +2 V, the spectra contains the blue copper hydroxide $Cu(OH)_2$, an orthorhombic system with lattice parameters a = 0.29490 nm, b = 1.05900 nm, and c = 0.52560 nm (ICSD[32] card 00-013-0420), and is missing the second of the two copper substrate peaks. The missing copper substrate peak is most likely due to the copper sheet, which is crystallographic textured, being rotated in XRD.

All of the samples had two small unknown peaks with constant intensity at 46 and 49°. These might be associated with impurities in the copper substrate.

Figure 12 shows the effect of temperature on the composition of the surface oxide. At higher temperatures, Cu_2O peaks at 30, 37, 42, and 62° grew higher due to the thermo-activated growth of cuprous oxide and the increase of thickness (see Fig. 6). At 85°C, an additional unknown peak at 20° also appears. The two small unknown peaks at 46 and 49° are present at all temperatures.

The GAXRD showed that the composition of surface oxide was mainly Cu_2O with no CuO. This result agrees with Raman spectroscopy results (not shown) but disagrees with XPS results. Figure 13 shows in the XPS Cu $2p_{3/2}$ spectrum for copper anodized at +3 V, 75°C, $t_1 = 10$ s and $t_2 = 60$ s. The peak position and the satellites indicate that both Cu_2O and CuO exist on the outer surface of copper oxide (no sputtering). However after sputtering, there was no CuO detected deeper in the oxide. The CuO was probably only a

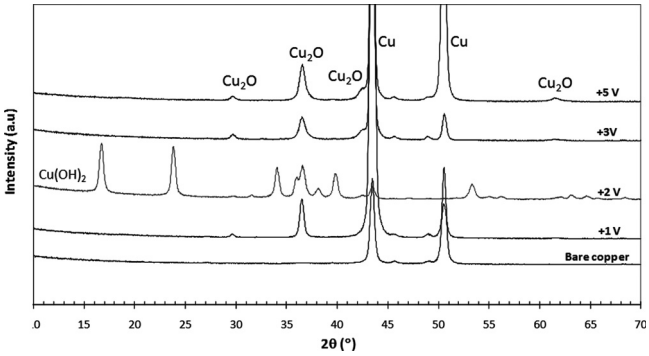

Figure 11. Effect of potential on GAXRD pattern of polycrystalline copper electrode anodized at 65°C with $t_1 = 10$ s and $t_2 = 60$ s.

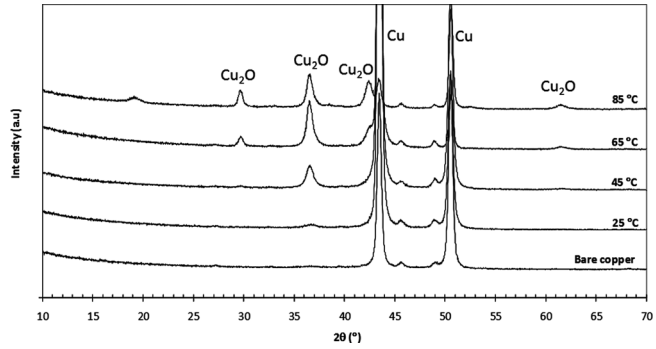

Figure 12. Effect of temperature on GAXRD pattern of polycrystalline copper electrode anodized at +3 V vs copper with $t_1 = 10$ s and $t_2 = 60$ s.

monolayer on the outer most surface which was not detectable by the GAXRD.

The proposed mechanism for the formation of the Cu_2O is shown below. During the transpassive polarization (t_1), there is a rapid dissolution of the copper as copper (II) as shown in Eq. 2, and oxygen evolution with acidification, as shown in Eq. 3 and Fig. 14a

$$Cu \rightarrow Cu^{2+} + 2e^- \quad [2]$$

$$2H_2O \rightarrow O_2 + 4H^+ + 4e^- \quad [3]$$

The acidification aids in the dissolution of the copper surface. The copper cations react with the hydroxyl anions in the solution to form the bicuprite ion complex as shown in Eq. 4. The bicuprite ion also has a blue color according to Pourbaix,[33] which agrees with the dark blue color of the NaOH electrolyte during the tests

$$Cu^{2+} + 3OH^- \rightarrow HCuO_2^- + H_2O \quad [4]$$

During time t_2 when the applied potential had been turned off, the bicurpite ion decomposed into Cu_2O with oxygen evolution via one or both of the chemical reactions shown in Eqs. 5 and 6, and then the Cu_2O deposited onto the surface as shown in Fig. 14b. Since we did not observe oxygen bubbles on the surface during time t_2, we propose that the Cu_2O formed in the solution and then deposited onto the surface

$$2HCuO_2^- + 2H^+ \rightarrow Cu_2O + 2H_2O + \tfrac{1}{2}O_2 \quad [5]$$

$$2HCuO_2^- \rightarrow Cu_2O + 2OH^- + \tfrac{1}{2}O_2 \quad [6]$$

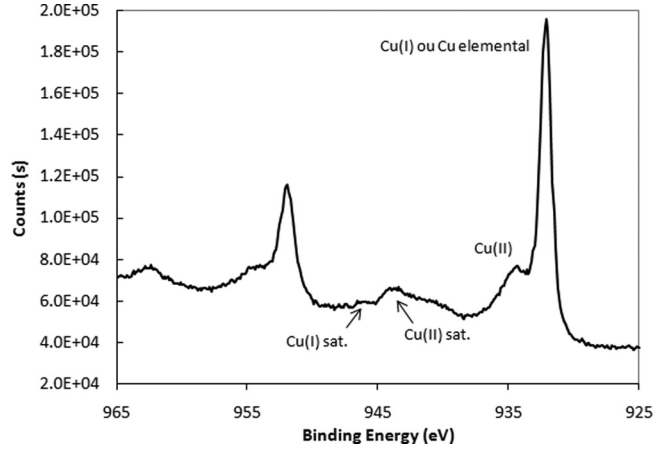

Figure 13. Cu $2p_{3/2}$ XPS spectrum of a polycrystalline copper electrode anodized at +3 V, 75°C, $t_1 = 10$ s and $t_2 = 60$ s.

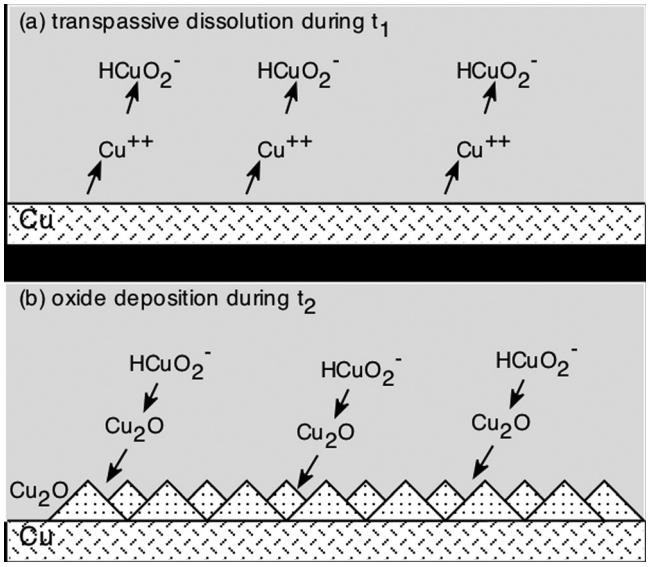

Figure 14. (a) Copper dissolves into the solution during the transpassive dissolution time t_1. (b) Bicuprite ions decompose and deposit Cu_2O onto the surface during time t_2.

Tests were also conducted to measure and improve the adherence and the corrosion resistance of these films. The oxide films showed relatively good adherence to the base copper, with no loss when adhesive tape was peeled from the surface, nor any loss by rubbing with a cotton swab. However the films did not exhibit improved corrosion resistance, nor did they show good resistance to repeated hand contact.

Conclusions

Copper polarization in concentrated NaOH (19 M, $p\mathrm{H} = 15.3$) showed the existence of several domains between +1 and +5 V/versus copper. Between +1 and +2 V versus copper, the oxide is dark gray or green and not esthetic with a precipitate of light blue $Cu(OH)_2$ forming on the surface at +2 V. In the transpassive domain (+3, +4, and +5 V versus copper), it was possible to deposit a Cu_2O layer with a bright and esthetic color range depending on the deposition conditions. Coloration depended mainly on the applied potential, the temperature of the solution, the time of anodization (t_1), and the time after anodization (t_2) when the oxide deposition occurred. The time t_2 has not been referenced in the literature, but was found to be a critical parameter for the growth, the thickness and the color of oxide on the copper substrate.

Cyclic voltammetry highlighted the complexity of electrochemical behavior of copper in the 19 M NaOH, in particular the appearance of an active dissolution peak A during the cathodic sweep, and an additional Cu^{III} peak (a_3) during anodization at 65 and 85°C, and that the potentials E_3, E_4, and E_5 belonged to transpassive region.

Glancing angle XRD demonstrated that the oxide formed after transpassive polarization was mainly composed of Cu_2O, regardless of the anodic potential from +3 to +5 V, and the temperature, from 25 to 85°C. These results were also confirmed by Raman spectroscopy. Thus color differences were due to differences in porosity, and roughness, and thickness.

In summary, an electrochemical process has been described to form an attractive and reproducible copper oxide on copper by controlling the four parameters (E, T, t_1, and t_2).

Acknowledgments

The authors thank James Michel and the Copper Development Association for funding this research. The authors also thank Virgil Lueth of the New Mexico Bureau of Geology & Mineral Resources for the GAXRD measurements, Dr. Shi for Raman measurements and Dr. Douglas Taylor for the ellipsometry measurements.

New Mexico Tech assisted in meeting the publication costs of this article.

References

1. O. Tissot, *Architecture: Atouts Cuivre,* European copper Institute, Brussels, Belgium (2005).
2. J. M. Taguri, M. B. I. Janjua, and W. C. Cooper, *Electrodeposition Surf. Treat.*, **1**, 77 (1972).
3. H. A. Miley, *J. Am. Chem. Soc.*, **59**, 2626 (1937).
4. D. B. Allred, *Electrochem. Soc. Interface*, **15**, 49 (2006).
5. G. Wyszecki and W. S. Styles, *Color Science: Concepts and Methods, Quantitative Data and Formulae*, Wiley Interscience, New York (1982).
6. K. Massau, *The Physics and Chemistry of Colors*, Wiley Interscience, New York (1983).
7. H. Y. H. Chan, C. G. Takoudis, and M. J. Weaver, *J. Phys. Chem. B*, **103**, 357 (1999).
8. D. Reyter, M. Odziemkowski, D. Belanger, and L. Roue, *J. Electrochem. Soc.*, **154**, K36 (2007).
9. F. Caballero-Brionesa, A. Palacios-Padrósa, O. Calzadilla, and F. Sanz, *Electrochim. Acta,* **55**, 4353 (2010).
10. J. P. Lorimer, T. J. Mason, M. Plattes, and D. J. Walton, *J. Electroanal. Chem.*, **568**, 379 (2004).
11. J. P. Lorimer, T. J. Mason, M. Plattes, S. S. Phull, J. Iniesta, and D. J. Walton, *Ultrason. Sonochem.*, **11**, 223 (2004).
12. M. Biton, G. Salitra, D. Aurbach, P. Mishkov, and D. Ilzycer, *J. Electrochem. Soc.*, **153**, B555 (2006).
13. A. Jagminas, J. Kuzmarskyte, and G. Niaura, *Appl. Surf. Sci.*, **201**, 129 (2002).
14. G. Jerkiewicz, B. Zhao, S. Hrapovic, and B. L. Luan, *Chem. Mater.*, **20**, 1877 (2008).
15. S. M. Abd el Haleem and B. G. Ateya, *J. Electroanal. Chem.*, **117**, 309 (1981).
16. J. Kunze, V. Maurice, L. H. Klein, H. H. Strehblow, and P. Marcus, *J. Phys. Chem. B*, **105**, 4263 (2001).
17. L. D. Burke, M. J. G. Ahern, and T. G. Ryan, *J. Electrochem. Soc.*, **137**, 553 (1990).
18. A. C. Cascalheira and L. M. Abrantes, *Electrochim. Acta*, **49**, 5023 (2004).
19. J. B. He, D. Y. Lu, and G. P. Jin, *Appl. Surf. Sci.*, **253**, 689 (2006).
20. S. Hrapovic, B. L. Luan, M. D. Amours, G. Vatankhah, and G. Jerkiewicz, *Langmuir*, **17**, 3051 (2001).
21. H. L. Wu, Y. L. Cheng, L. L. Li, Z. H. Chen, H. M. Wang, and Z. Zhang, *Appl. Surf. Sci.*, **253**, 9387 (2007).
22. Y. T. Sul, C. B. Johansson, Y. Jeong, C. B. Johansson, and T. Albrektsson, *Med. Eng. .Phys.*, **23**, 329 (2001).
23. S. Van Gils, P. Mast, E. Stijns, and H. Terryn, *Surf. Coat. Technol.*, **185**, 303 (2004).
24. H. El-Sayed, M. T. Greiner, and P. Kruse, *Appl. Surf. Sci.*, **253**, 8962 (2007).
25. A. Belwalkar, E. Grasing, W. Van Geertruyden, Z. Huang, and W. Z. Misiolek, *J. Membr. Sci.,* **319**, 192 (2008).
26. R. Babic′, M. Metikoš-Hukovic′, and A. Jukic′, *J. Electrochem. Soc.,* **148**, B146 (2001).
27. E. Jackson, *Hydrometallurgical Extraction and Reclamation*, p. 46, Harwood, Chichester, NY (1986).
28. H. Demir, O. Kucuk, C. Ozmetin, and M. M. Kocakerim, *Chem. Eng. Process.*, **44**, 895 (2005).
29. M. Z. Zhang, M. Wang, Z. Zhang, J. M. Zhu, R. W. Peng, and N. B. Ming, *Electrochim. Acta*, **49**, 2379 (2004).
30. N. Liu, D. Wu, H. Wu, C. Liu, and F. Luo, *Mater. Chem. Phys.*, **107**, 511 (2008).
31. Y. Zhou and J. A. Switzer, *Scr. Mater.*, **38**, 1731 (1998).
32. Inorganic Crystal Structure Database (ICSD), FIZ Karlsruhe, Hermann-von-Helmholtz-Platz 1, 76344 Eggenstein-Leopoldshafen, Germany, helpdesk@fiz-karlsruhe.de.
33. M. Pourbaix, *Atlas of Electrochemical Equilibria in Aqueous Solutions*, NACE Houston, TX (1974).